ELSEVIER

Tectonophysics 352 (2002) 257–274

TECTONOPHYSICS

www.elsevier.com/locate/tecto

Microstructural observations on natural syntectonic fibrous veins: implications for the growth process

Christoph Hilgers *, Janos L. Urai

Geologie–Endogene Dynamik, RWTH Aachen, D-52056 Aachen, Germany

Received 19 July 2001; accepted 5 April 2002

Abstract

Syntectonic antitaxial and ataxial fibrous veins were investigated using SEM, microprobe, cathodoluminescence (CL) and optical microscopy. In antitaxial calcite veins, fibres and surrounding selvage grew simultaneously, with similar growth rates of crystallographically differently oriented grains. New material precipitated at the vein margin in antitaxial and bi-mineralic ataxial microstructures. Bridges of country rock material formed during vein growth in an initial en-echelon vein system. In our antitaxial and bi-mineralic ataxial samples, the spacing of solid inclusions does not reflect individual crack-seal openings.

Keywords: Crack-seal; Fibrous vein; Antitaxial; Ataxial; Cathodoluminescence

1. Introduction

In structural geology, early observations of some types of syntectonic fibrous veins were interpreted to have formed by growth, with the fibre grain boundary tracking the instantaneous opening direction (Taber, 1916; Grigorev, 1961). Renewed interest started with Durney (1972) and Durney and Ramsay (1973), who used fibrous veins to deduce progressive deformation from rocks (Ramsay and Huber, 1983). Since then, detailed field studies and numerical modelling have helped to better constrain the applicability of the technique (Cox, 1987; Cox and Etheridge, 1983; Urai et al., 1991; Spencer, 1991; Dijk and Berkowitz, 1998; Koehn et al., 2000; Hilgers et al., 2001), although rigorous tests of the mechanism are still lacking.

For fibrous microstructures, Durney and Ramsay (1973) introduced the microstructural terms syntaxial, antitaxial and stretched crystals. Passchier and Trouw (1996, p.135) proposed the term ataxial for stretched crystals (Fig. 1). Recently, the confusing nomenclature of vein fill microstructures was extensively discussed in Bons (2000). For the convenience of the reader, we will explain the main terms.

In *antitaxial* veins, material precipitates at the vein–wall interface. Thus, microstructures have grown from the vein centre towards the wall. A *median line* often marks the vein's centre, which generally is an accumulation of numerous small calcite grains, rapidly outgrown during initial vein development. The vein material precipitated can be of different composition than the country rock, with a discontinuity between vein and host rock. Our anti-

* Corresponding author.
E-mail address: c.hilgers@ged.rwth-aachen.de (C. Hilgers).

0040-1951/02/$ - see front matter
PII: S0040-1951(02)00185-3

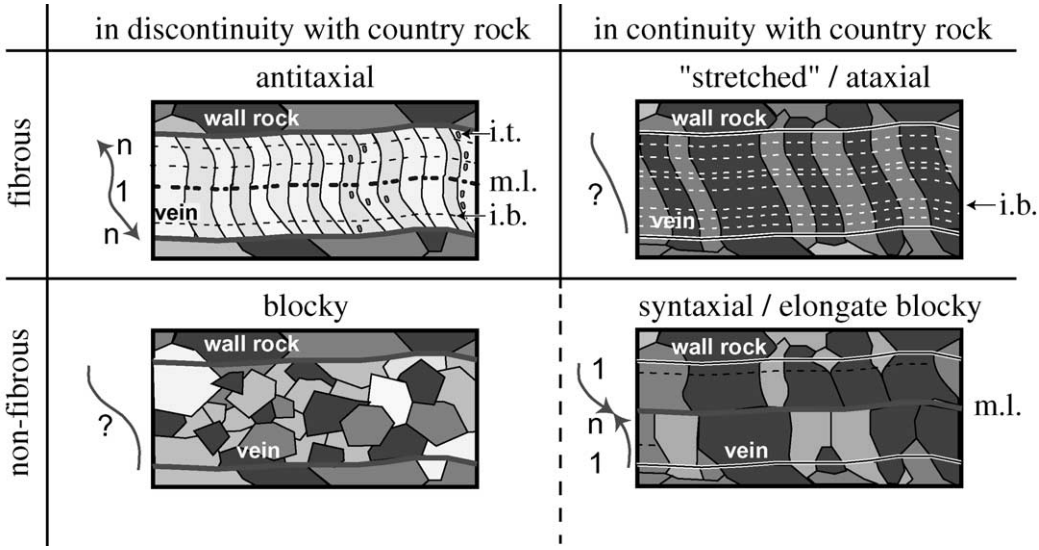

Fig. 1. Classification of the published nomenclature with respect to the grain morphology and the crystal growth process. Lines/arrows represent the opening direction. The centre of syntaxial and antitaxial veins often shows a central median line (m.l.). Note that we use the following terms to describe the arrangement of inclusions: Inclusion bands (i.b.) are arranged parallel to the vein–wall interface. Inclusion trails (i.t.) extend subnormal to the vein–wall or are distributed irregularly across the veins. Blocky vein microstructures can both overgrow from the country rock and nucleate in the vein.

taxial calcite veins are usually found in slates, and are always surrounded by a small quartz *selvage* between vein and country rock (see also Williams and Urai, 1989). The fibre grain boundaries are smooth, often curved, but grains are *optically continuous* across the vein.

Ataxial fibres cross the vein from one wall to the other, and are optically continuous. In contrast to antitaxial veins, they are epitaxial overgrowths of the country rock grains, with sometimes serrated grain boundaries. These veins often contain solid inclusions arranged parallel to the vein–wall interface.

Within the vein, small particles of different composition are sometimes arranged as *inclusion bands* or inclusion *trails* (Ramsay, 1980) (Fig. 1). These particles can be fragments of the country rock, newgrown minerals or fluid inclusions.

It is obvious from most veins that they formed in a dilation site with vein material precipitated in a void (Anonymous, 1814), rather than being a replacement feature, because markers on either side of the vein match when closing the vein structure (Dunne and Hancock, 1994).

A range of different scenarios has been proposed for the kinematics of the opening process. Quasi-continuous precipitation with an accretion site of molecular dimensions (Durney and Ramsay, 1973; Fisher and Brantley, 1992; Bons and Jessell, 1997; Means and Li, 2001; Wiltschko and Morse, 2001) forms an end-member of a series where the other extreme is vein formation where accretion takes place in steps (discrete opening and precipitation, crack-seal; Hulin, 1929; Ramsay, 1980).

In syntectonic vein growth, the key parameter which controls crystal morphology is the ratio of crystal growth velocity versus opening velocity, and the width of the opening increment (Mügge, 1928; Hilgers et al., 2001). When opening is faster than growth, the grains grow as in a free fluid with corresponding microstructures.

For the crack-seal mechanism, the width of individual cracks has been correlated with the inclusion spacing in the vein (both inclusion trails and bands; Cox and Etheridge, 1983; Cox, 1987, 1995; Fisher and Brantley, 1992; Fisher et al., 1995), with typical values between 4 and 200 μm.

The aim of this study is to present a detailed characterisation of natural antitaxial and ataxial syntectonic fibrous veins and draw conclusions on the process of formation. Notes of caution are added

concerning the usage of inclusion trails and bands as indicator for crack-seal vein growth.

2. Sample area

Syntectonic antitaxial calcite fibres were sampled in the Tertiary flysch of the Morcles nappe, Switzerland, in Palaeozoic slates in upper New York State, USA, and Palaeozoic slates in the Rocky Mountains, Canada (see Table 1 for detailed description of locations). These areas were chosen because of the known presence of antitaxial veins, and to allow a comparison of the microstructures formed in different regional settings.

Table 1
Description of the location of antitaxial and ataxial fibrous veins

Switzerland (antitaxial calcite fibres and bi-mineralic ataxial veins)

- Swiss Grid 562.5 108, Tertiary flysch of the Morcles nappe, around lake Salanfe, about 7 km NW of Martigny. Black slates (antitaxial samples) and siltstones (ataxial samples), about 20 m above the Morcles thrust. Sample and thin section number CH-99*x*, CH-98*x*.
- Swiss Grid 733 197.5, Upper Cretaceous–Eocence Flysch near the Glarus thrust, about 1 km E of Elm. Antitaxial calcite vein in black slate. Sample and thin section number CH-01-*x*.

United States (antitaxial calcite fibres)

- 43°33.62′N, 73°19.33′W, dismantled quarry on the N side of highway 4 about 4 km E of Whitehall/New York State, near the border to Vermont. Black slates of the Cambrian Hatch Hill formation in the Taconic Allochthon, about 900 m above the Taconic frontal thrust (Kidd and Means, personal communication, 2000). Sample and thin section number NY-*x*.

Canada (antitaxial calcite fibres)

- 51.5°N 117.8°W, roadcut when crossing the Columbia river, SE of Golden/day 1 stop 5 of CTG Nuna field trip 1998. Black slates of the Cambro-Ordovician McCay Group, about 600 m below the Purcell thrust (Simony, 1998). Sample and thin section number Ca-*x*.

Germany (ataxial quartz fibres)

- Gauβ-Krüger $R^{25}30$ $H^{56}13$, Lower Devonian sandstones of the Siegenian Rurberger formation on the shore of the Rur lake/water reservoir about 1.5 km SE of Schmidt. Sample and thin section number R-*x*, 6 km SE of the Eifel nappe.
- Mosel Valley, roadcut $R^{25}79.5$ $H^{55}44.8$ Lower Devonian sandstones (Lower Emsian, Singhofen formation), 3 km SW of Alf. Sample and thin section number Mo-*x*.

x refers to individual sample numbers in the figure captions.

Bi-mineralic ataxial veins were sampled in flysch siltstones of the Morcles nappe, and mono-mineralic ataxial veins in the Palaeozoic sandstones around the Rur lake and the Mosel valley, Germany. All areas expose rocks of lower greenschist facies.

3. Analytical techniques

When possible, samples were cut carefully parallel to the plane defined by curved fibres (thus, the thin sections contained the whole curved fibre). This was usually a section almost normal to foliation. Alternatively, some veins were cut normal to the fibre long axis. Double-polished ultra-thin sections were studied in optical microscopy, cathodoluminescence (CL), and microprobe.

For cathodoluminescence studies, we used the hot CL (type: HC-1 LM, company: Neuser, Bochum, Germany) run at a voltage of 14 kV with a beam current density of 0.6–0.75 mA/mm^2. Microprobe work was based on a mapping technique using a Cameca Camebax microprobe with 1-μm spot size, 3-μm grid spacing, 15-kV acceleration voltage and 50-mA beam current. For SEM, samples were polished and etched with dilute HCl, exposing calcite grain boundaries and the shape of the wall (Hilgers et al., 2001).

4. Antitaxial veins

Detailed observations showed that the microstructures in the samples are quite similar. Description, however, is made always with reference to a particular sample, indicated in the figure caption.

4.1. Macroscopic observations

In all samples, country rock containing antitaxial veins consists of fine-grained black slate with up to a few millimeters-thick quartz–calcite interlayers, which provide markers for correlation of material positions on both sides of the vein. All antitaxial calcite veins within the slate are oriented sub-normal to bedding, sub-parallel to each other. Veins are often isolated from each other in 2-D sections parallel and normal to bedding (Fig. 2a–c). Serial sectioning has

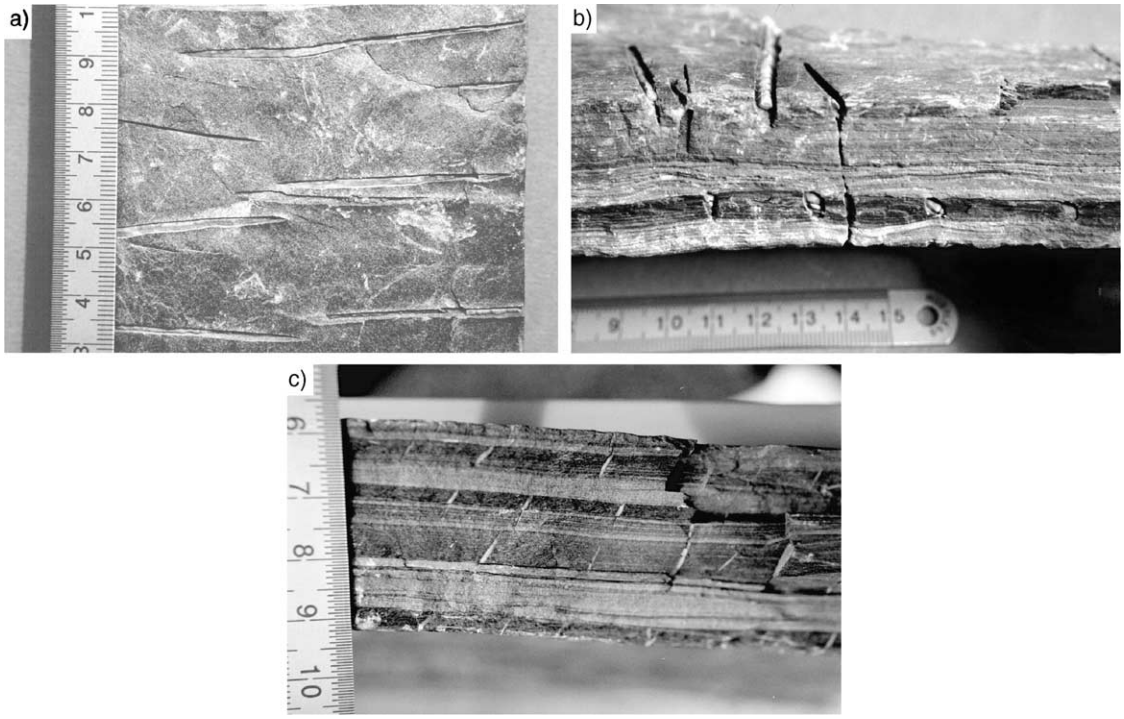

Fig. 2. Hand specimens of antitaxial calcite veins in black slate. Scale in centimetres. (a) Veins viewed on bedding, sample CH-98. (b) Oblique view onto sample CH-990822-W1. Veins are limited to beds of black slate and end in the third dimension. (c) Beds of black slates contain most calcite veins, which abut against the bright quartz–calcite beds, sample CH-9908A.

shown that at least some of the antitaxial fibrous veins are fully isolated in three dimensions.

Mostly the veins within the slate abut against the quartz–calcite beds (Figs. 2b–c and 3b,e), only wide veins crosscut such layers (Fig. 3a). A few antitaxial calcite veins are located in the quartz–calcite beds (Fig. 3a). Quartz–calcite-rich beds above and below a vein become slightly thinner at the vein-bedding intersection (Fig. 2b).

4.2. Petrography

4.2.1. Vein

Ultra-thin sections were prepared from samples cut parallel to 2-D curved antitaxial fibres. All calcite fibres extend across the vein (Fig. 3). The vein's centre sometimes displays a median line, defined by fine-grained calcite grains, fluid inclusion lines, or wall rock particles (Figs. 3e,f and 4b,c) (see also Urai et al., 1991). All calcite fibres curved in two dimensions connect markers such as bedding on both sides of the wall (Figs. 3 and 4). 3-D curved grain boundaries were not used for checking the tracking criterion, because single fibre grain boundaries cannot be traced across the vein using 2-D thin sections.

Calcite fibres connect fractured quartz grains on either side of the vein (Fig. 4a,b). Inclusion lines in the quartz grain show healed microcracks oriented sub-parallel to the vein–wall (Fig. 4a,b). Although the optical orientation and general habit of the corresponding quartz grain on either side of the vein do coincide, the vein–wall interface does not match due to overgrowth of quartz.

Fibres are optically continuous across the median line towards the walls in all clear 2-D sections. The fibre width of the samples investigated varies from 10 to 350 μm. The calcite veins contain straight twin lamellae, which are concentrated in the vein's centre and diminish towards the vein–wall interface (Fig. 4c). This indicates fibres being less strained in the outer, youngest part of the vein.

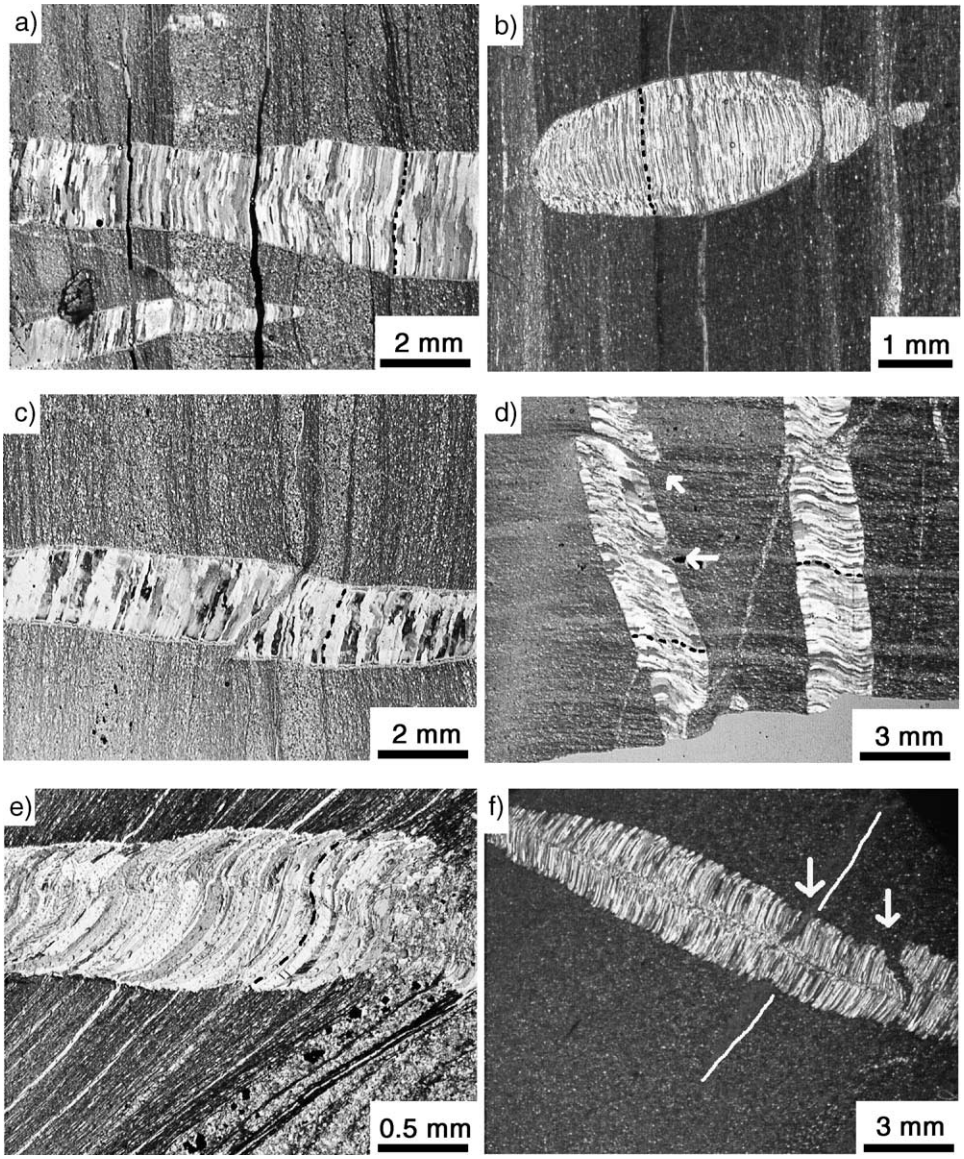

Fig. 3. Micrographs of antitaxial calcite fibres in black slate cut normal to bedding. All vein fibres connect bedding on both sides of the vein. Dashed line—trace of a fibre grain boundary. (a) The wide vein crosscuts the vertical, calcite-rich bedding, but becomes thinner in this zone. Small veins are located in this calcite-rich bed in the top of the image, thin section NY-36. (b) The vein is surrounded by country rock in this section, normal to bedding. It abuts against the calcite-rich bedding on the left side. On the right hand side, the vein disappears when it reaches the thin quartz–calcite rich bed, but continues after this zone, thin section CH-980802-6. (c) A small bridge of wall rock crosses the vein in the centre of the image, thin section NY-19A. (d) Small fragments of wall rock protrude into the vein (arrows), thin section CH-98-H01. (e) Strongly, symmetrically curved fibre grain boundaries with most grains having optical continuity across the vein, sample NY-2. (f) Wall rock fragments protrude into the vein, curved in different directions (arrows). The white lines mark bedding, thin section CH-01A.

Antitaxial calcite–calcite fibre grain boundaries are not serrated but smooth along their long axis (Figs. 3 and 4) up to the limit of observation, a magnification of × 10.000 (Fig. 6e). Sections normal to the fibres show grain boundaries with slightly curved, serrated grain boundaries (Fig. 5d). The vein

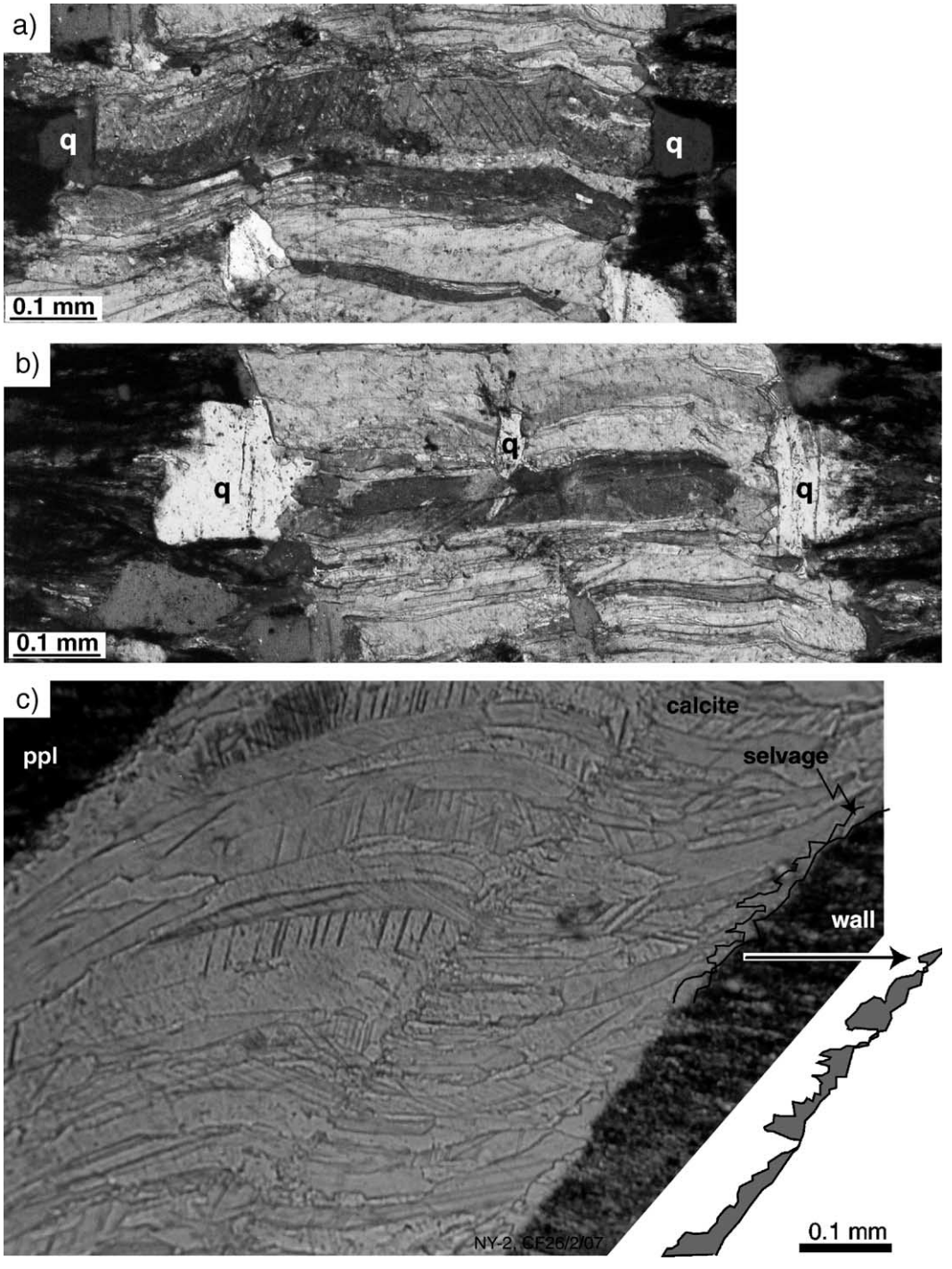
a)
q
q
0.1 mm
b)
q
q
q
0.1 mm
c)
ppl
calcite
selvage
wall
NY-2, CF26/2/07
0.1 mm

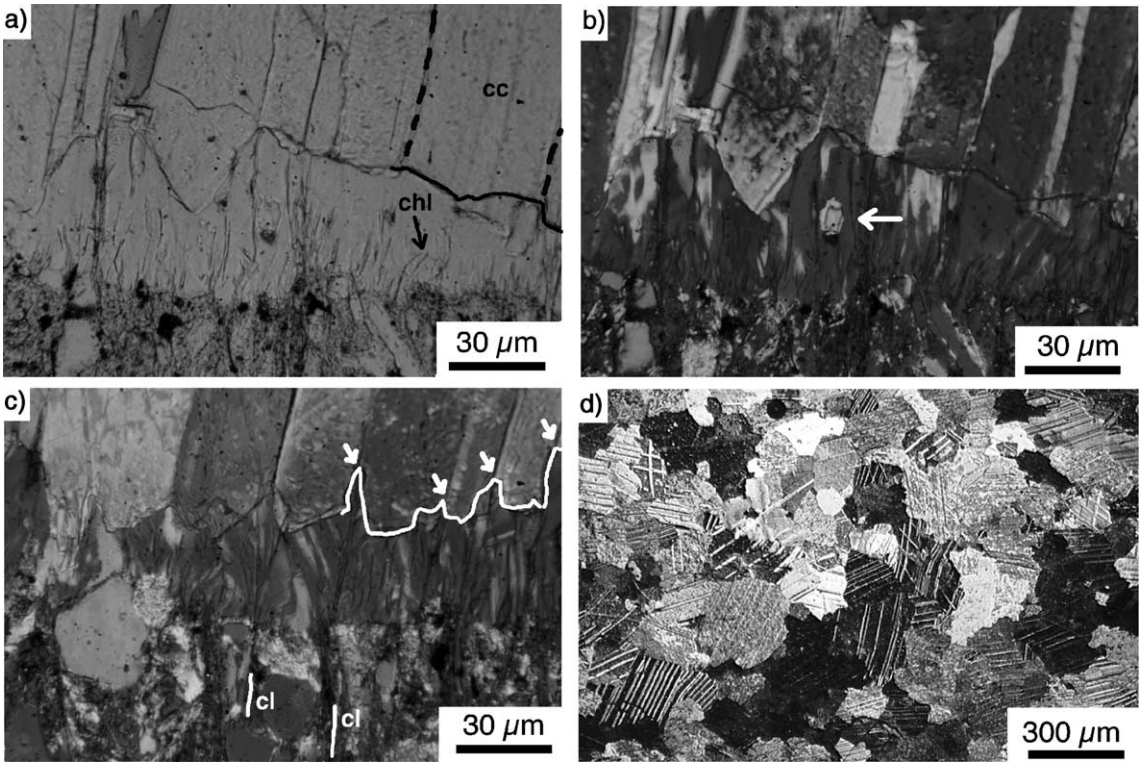

Fig. 5. Details of the vein–wall interface of sample NY-36. (a) Interface between vein (top) and country rock (bottom of image) in plane polarised light. In contrast to the wall–selvage interface, the selvage–vein interface is very rough. Chl—chlorite, cc—calcite, black line—selvage–vein interface, dashed lines—fibre grain boundaries. (b) A small fragment of calcite is embedded in the quartz selvage (arrow). Same as (a), with gypsum and crossed polarises. (c) Cleavage planes in the country rock continue across the quartz selvage. Note that fibre grain boundaries are located at peaks of the selvage (arrows) and correspond with the location of cleavage planes in the country rock. cl—cleavage in the country rock; gypsum and crossed polarisers. (d) Thin section cuts normal to the fibre long axis (sample NY-32). The fibre grain boundaries are serrated, the vein is non-porous, and twin lamellae illustrate the different crystallographic orientation of the grains in this microstructure.

microstructure is completely sealed without any porosity observed in thin sections.

A thin quartz selvage is located between the antitaxial vein and the country rock (Fig. 4c, lower right). Against the selvage–vein interface, fibres often develop straight boundaries (Fig. 5a–c).

Wall material protruding into the vein curves parallel to the fibre orientation (Fig. 6a,b,d), identified as quartz selvage in BSE mode. A different type of protrusions consists of country rock, which sometimes continues across the vein (Fig. 6d) and forms bridges (Nicholson and Ejiofor, 1987; Nicholson, 1991) (marked by arrows in Fig. 3c,d,f). In such protrusions, mica was observed to extinct undulose, indicating deformation.

4.2.2. Vein inclusions

Antitaxial calcite fibres contain solid inclusion trails, which are host rock fragments and new-grown chlorite. Chlorite flakes are located inside the selvage

Fig. 4. (a, b) Fractured quartz grains of the country rock indicate a well-consolidated rock before rupture (sample CH-98MB). In all cases, fibre grain boundaries connect the fractured quartz on both sides of the vein. The sample was kindly provided by Martin Burkhard; q—quartz. (c) Image in plane polarisers, showing the decrease of twinning intensity from the vein centre towards the margin. The interface between vein and country rock consists of a thin quartz selvage with varying width, sketched on the right hand side. While the interface between selvage and country rock is relatively smooth, the amplitude of the selvage–vein interface is much higher, sample NY-2.

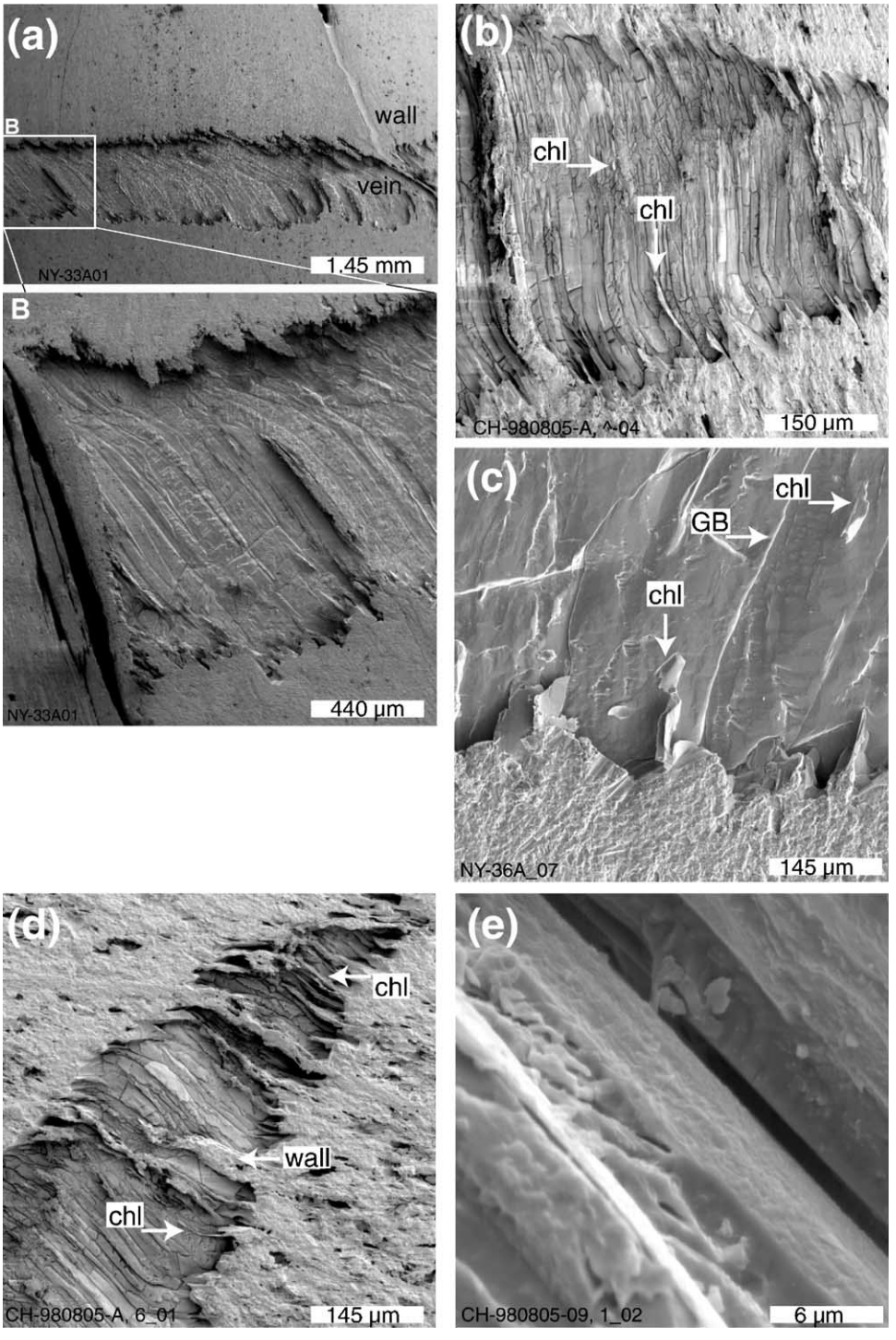
(a)
B
wall
vein
NY-33A01
1.45 mm
B
NY-33A01
440 µm
(b)
chl
chl
CH-980805-A, ^-04
150 µm
(c)
chl
GB
chl
NY-36A_07
145 µm
(d)
chl
wall
chl
CH-980805-A, 6_01
145 µm
(e)
CH-980805-09, 1_02
6 µm

(Figs. 5a and 7a), some chlorite is embedded in the vein (Fig. 6b) and crosses the vein's tip (Fig. 6d). Chlorite (001)-planes are aligned parallel to the fibre curvature (Fig. 6b,d). Inclusion trails or bands composed of quartz selvage were never found within the veins, rarely small quartz fragments float within the vein (Fig. 7b,c).

4.2.3. Selvage

Antitaxial calcite veins are frequently surrounded by a selvage with a width of about 30 μm. The selvage consists of quartz fibres and chlorites (Figs. 5a and 7a).

The morphology of the selvage has a much larger amplitude along the vein–selvage interface than that of the wall–selvage interface (Figs. 5a and 7a). As a result, the selvage is thickest in the region of a fibre–fibre grain boundary (Figs. 4c and 7a). These peaks of the selvage coincide when correlated across the vein (Fig. 6a,b,d; Fig. 2c in Hilgers et al., 2001). Vein fibre grain boundaries are located at peaks (Figs. 5c and 6c) (cf. grain boundary attractors in Hilgers et al., 2001). The fibrous to elongate-blocky quartz grains in the selvage show growth competition with a decreasing number and a widening of grains towards the vein–selvage interface (Fig. 5b,c). Often, quartz grain boundaries are oriented normal to the selvage–vein interface (Fig. 5c) (Hilgers and Urai, 1999; Koehn, personal communication). Occasionally, very small calcite grains are embedded in the selvage (Fig. 5b). This selvage at the vein–wall interface curves opposite to the fibre grain boundaries (Figs. 6a–d and 7a).

4.3. Cathodoluminescence

Many veins exhibit a discontinuity in the CL intensity pattern (Urai et al., 1991). The CL-banding is aligned sub-parallel to the wall, parallel to a median line and not related to any crystallographic orientation of vein calcite fibres. The parallelism of the median line and CL-banding suggests the same growth rate of differently oriented calcite crystals (Fig. 7d–g).

CL-banding shows a rough morphology, which neither matches with its counterpart on the other side of the vein, nor with the vein–selvage interface (Fig. 7e). The amplitude of the roughness can be correlated with the amplitude of the vein–selvage interface. Where the banding crosscuts fibre grain boundaries, grain boundaries show no change in orientation (Fig. 7f,g). On a large scale, luminescence in the country rock exposes no evidence of any zonation around the lens-shaped veins investigated (Fig. 7h).

4.4. Microprobe data

Element distribution maps based on X-ray intensity mapping with a microprobe allow semi-quantitative analysis of the selvage, vein and country rock (Fig. 8).

The distribution of Mg and Al/K shows that chlorite is present both within the selvage and in the vein. Chlorite flakes crosscut the selvage and reach into the vein, connecting host rock and vein (Fig. 8b,e). The spacing varies between different chlorite inclusion trails and cannot be correlated with any feature parallel to the vein–wall, which might indicate crack-seal increments.

Inclusion trails of chlorites are not aligned parallel to the curved fibre grain boundary, but are distributed irregularly across the vein (Fig. 8). Their abundance increases parallel to the vein–wall interface in a zone, where a change in concentrations of Mn and Mg is visible (Fig. 8d,e). This change in concentration corresponds to the CL-banding presented in Fig. 8a.

Concentration of Ca changes along the vein–wall interface, the variation corresponding to individual calcite fibres (Fig. 8c). Enriched Al/K and Mg concentrations outline cleavage zones in the host rock (Fig. 8b).

Fig. 6. SEM images (secondary electrons) of etched antitaxial calcite veins. (a) The vein–selvage interface is rough, with peaks of the wall curved in the same direction as the calcite fibres in the vein, sample NY-33. (b) Chlorite plates (confirmed by EDX) are abundant at the vein–selvage interface, and are curved parallel to the calcite fibres. Again, the peaks of the wall are oriented in the same direction as the calcite fibres, sample CH-980805-A. (c) Fibre grain boundaries are located at peaks of the selvage. The curved grain boundary (GB) is smooth. Chlorite plates extend from the selvage into the vein (a chlorite plate is incorporated in the vein on the upper right of the image), sample NY-36A. (d) Detail of the tip of a vein, where country rock crosscuts the vein. The curvature of wall rock protrusions and chlorite is parallel to that of the calcite fibres, sample CH-980805-A. (e) Close-up of a fibre grain boundary, which is smooth between adjacent fibres, sample CH-980805-09.

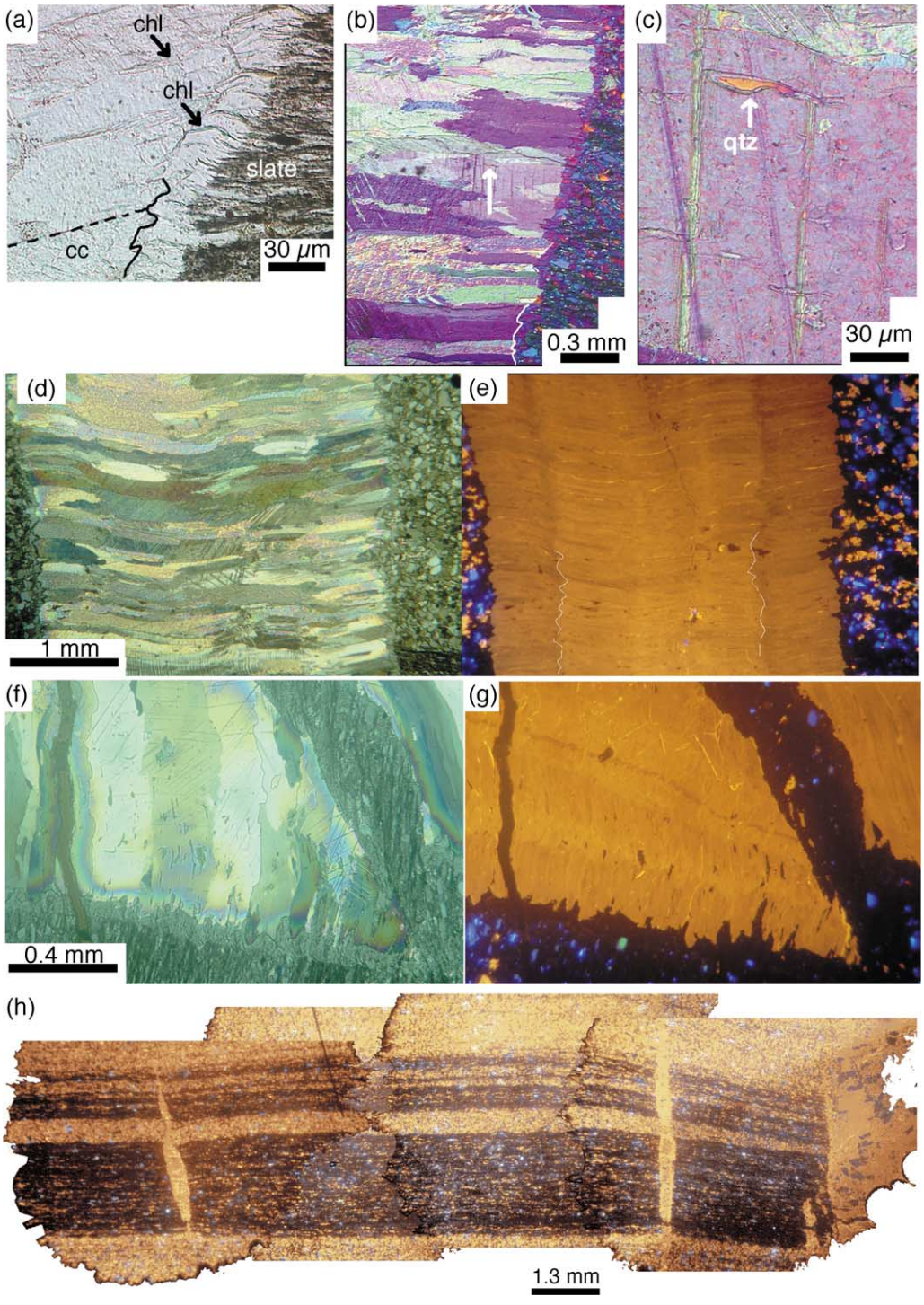
(a)
chl
chl
slate
cc
30 μm
(b)
0.3 mm
(c)
qtz
30 μm
(d)
1 mm
(e)
(f)
0.4 mm
(g)
(h)
1.3 mm

5. Ataxial veins

5.1. Macroscopic observations

Our ataxial veins are arranged normal to bedding and sub-parallel to each other. They were found in slaty siltstone and fine-grained marls, but never in fine-grained black slate. The veins are composed of bi-mineralic quartz and calcite fibres (quartz and calcite; Morcles nappe), or mono-mineralic quartz of samples from the Rur lake and the Mosel valley, where the wall rock is a quartzite.

5.2. Petrography

5.2.1. Vein

Our ataxial fibres never contain curved grain boundaries or a median line.

Bi-mineralic veins connect markers on both sides of the vein (Fig. 9a–d). Twin lamellae in bi-mineralic quartz–calcite fibres are straight. The fibre grain boundary is highly serrated along the fibre long axis. Quartz fibres are epitaxial overgrowths on the country rock grains (Fig. 9b), and widen slightly towards the vein centre (Fig. 9b,c).

In mono-mineralic ataxial veins, grain boundaries are smooth in quartz fibres (Fig. 9e–f). Ataxial fibres widen from the vein–wall interface towards the vein centre, with the number of grains decreasing towards the vein centre. A selvage is absent in all our ataxial microstructures.

5.2.2. Vein inclusions

Inclusion bands are present in ataxial quartz fibres of bi-mineralic quartz–calcite veins and mono-mineralic vein samples (Fig. 9). In bi-mineralic veins, these inclusion bands consist of solid material, and do not continue across the quartz–calcite fibre grain boundary (Fig. 9c,d). Spacing of inclusion bands in quartz fibres ranges between 5 and 15 μm and corresponds to the lower limit described by various authors for antitaxial quartz fibres (Cox and Etheridge, 1983; Cox, 1987, 1995). Small zones are inclusion-free within individual quartz fibres, arranged at the fibre margin parallel to the fibre long axes (Fig. 9c,d). Mono-mineralic veins generally show fluid inclusion bands crossing all fibres, sub-parallel to the vein–wall interface.

5.3. Cathodoluminescence

No discontinuity in luminescence was detected in bi-mineralic ataxial samples from the Morcles nappe, Switzerland and mono-mineralic veins around the Rur lake, Germany.

6. Discussion

The discussion will be focused on the growth history of anti- and ataxial veins, and on inclusion bands as indicators of crack-seal increments.

Fig. 7. (a) Vein–wall interface of an antitaxial calcite vein hosted in slate. The quartz selvage contains chlorite plates, growing from the wall towards the vein, as indicated by their abundance at this site. Chlorite plates are curved opposite to the fibre grain boundary (marked with a dashed line), being aligned parallel to the fibre at the vein–selvage interface. cc—fibrous calcite in the vein, chl—chlorite in the quartz selvage, black line—vein–selvage interface, sample CH-9908 B2. (b) Rarely quartz is included into the calcite fibres. The arrow points to such a tiny inclusion enlarged in the following micrograph. Crossed polarisers and gypsum plate, thin section NY-19A. (c) Detail of (b), showing a small inclusion of quartz in upper part of the image, elongated parallel to the fibre long axis. Inclusions are arranged in inclusion trails. Crossed polarisers and gypsum plate, thin section NY-19A. (d) Antitaxial calcite fibres twinned in the centre of the vein. Twinning intensity of calcite decreases from the vein centre towards the vein–wall interface. Crossed polarisers, thin section NY-36. (e) CL-image of (d). Amplitudes of the CL-banding are large and can be correlated with the roughness of the vein–selvage interface. The roughness of the CL-banding does neither match with its counterpart on the other side of the median line, nor with the vein–selvage interface. The morphology of the CL-banding is quite linear without any evidence of the banding following crystal facets of calcite, thin section NY-36. (f) Detail of an antitaxial calcite fibrous vein and its selvage. Crossed polarisers, thin section NY-19A. (g) CL image of (f). Fibre grain boundaries do not show a change in orientation or morphology in the region of CL-banding. Inclusion trails can be correlated with the banding. The banding trends oblique to the wall and ends in the tip of the vein. A country rock protrusion crosses the vein on the right hand side, and corresponds to the bridge shown in Fig. 3c, thin section NY-19A. (h) The luminescence in the wall around two small antitaxial calcite veins does not show any gradients, sample CH-980805/5.

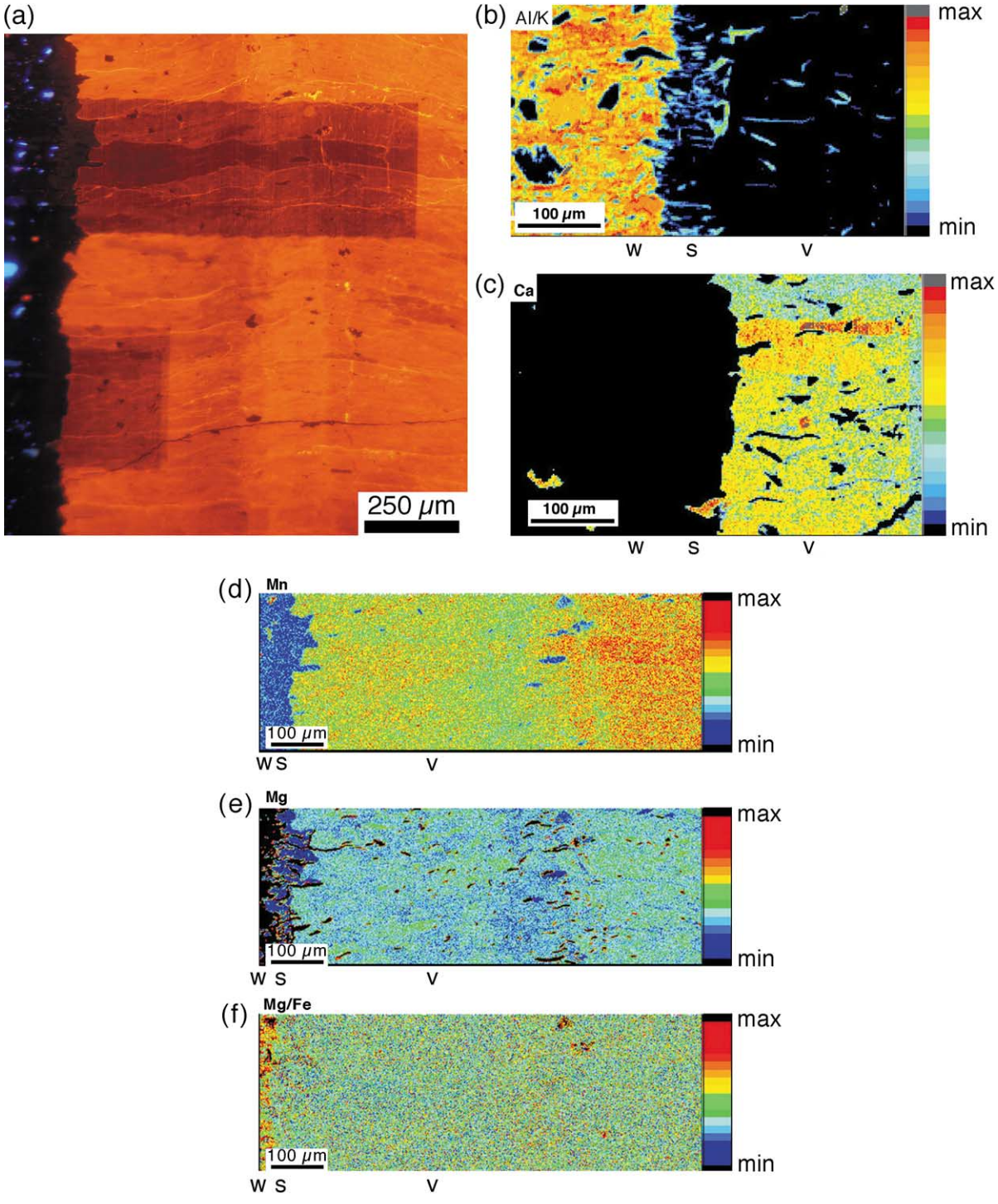
(a)
250 μm
(b) Al/K
max
min
100 μm
W S V
(c) Ca
max
min
100 μm
W S V
(d) Mn
max
min
100 μm
W S V
(e) Mg
max
min
100 μm
W S V
(f) Mg/Fe
max
min
100 μm
W S V

6.1. Antitaxial veins

The shape of CL-banding corresponds in amplitude to vein–selvage and not the wall–selvage amplitude. This suggests that (i) the morphology of this banding is a relict of an earlier selvage–vein interface, and (ii) the selvage was present at least during part of calcite vein growth. This interpretation is supported by the presence of chlorite in both quartz selvage and calcite vein, and some chlorites extending from the selvage into the vein. It requires chlorite growth during quartz selvage and calcite fibre formation. The abundance of chlorite at the selvage–wall interface and its extension from the wall into the selvage shows that it grew from the wall towards the vein. Quartz grew in the same direction, indicated by widening of grains towards the vein. Thus, we interpret selvage and vein to have grown simultaneously. Quartz and chlorite grain boundaries were shown to be oriented normal to the selvage–wall and selvage–vein interface (especially Figs. 5b,c and 7a). Such face-controlled growth requires the vein–calcite interface to be present during selvage formation.

Chlorite flakes are randomly distributed within the calcite vein. No path was observed along the vein–selvage interface without chlorite extending from the wall into the vein. Such an irregular pattern is difficult to interpret as a crack-seal process along the vein–selvage interface, with increments correlated to inclusion spacing. In contrast, chlorites appear to have grown from the selvage into the vein during vein growth.

Some veins are surrounded by country rock in 3-D, which allows us to make conclusions as to the transport mechanism. These veins have been filled from the matrix, and fluid did not use a fracture system. If the fluid entered the vein at its tip, we would expect a chemical gradient changing along to the vein–wall interface. Because concentration changes of Ca are limited to adjacent fibres (especially Fig. 8c) and CL intensity pattern changes parallel to the vein–wall, we suggest that the vein be filled from the side. Rye and Bradbury (1988) made similar observations of material flux from the wall. Based on the syn-growth origin of quartz selvage and the calcite vein, and low diffusivity of quartz–quartz grain boundaries, we infer that material entered the vein along chlorite–quartz interfaces in the selvage.

Calcite fibres are optically continuous across the vein and are curved in 2-D. The absence of any new grains within the vein suggests that no grains were nucleated during vein growth after the initial formation of calcite in the vein centre/median line. This implies that supersaturation was sufficiently low at the site of growth (the selvage–vein interface) (Kleber, 1983, p. 181; Mullin, 1993, p. 185). No indication of CL-banding tracing individual calcite facets was observed in our samples. If calcite grains grew in a free fluid, a change in fluid composition (causing CL-banding) would result in luminescence gradients, which outline the facets of individual grains (ten Have and Heijnen, 1985). Due to the lack of such observations, the development of facets on fibre crystals must have been suppressed during vein formation. Differently oriented fibres grew with similar growth rates, as indicated by the linear CL-banding and the absence of growth competition. This coincides with numerical modelling (Urai et al., 1991; Hilgers et al., 2001), which suggests that the development of facets and growth competition is suppressed, if the opening increments of the vein are small. The fibre grain boundaries are located at selvage peaks, the latter being aligned parallel to the orientation of the fibre grain boundaries (i.e. SEM images in Fig. 6). These peaks consist of selvage material, with the internal structure in the selvage often observed to be oriented normal to the vein–selvage interface (e.g. Fig. 7a). Curvature of selvage peaks and calcite fibres suggests coupling of selvage and vein. In the case of mechanical coupling, we would expect some deformation in the selvage and the vein, but clear indicators are missing. Hilgers et al. (2001) pointed out that fibres

Fig. 8. Microprobe map of thin section NY-36 (Fig. 7d, e) showing details of the vein–wall interface. The country rock is located on the left hand side of the image. (a) CL-image indicating the location of the two microprobe maps shown in Fig. 9b–f. (b) The distribution of Al/K marks the cleavage planes in the country rock, and shows chlorites crossing the quartz selvage. (c) The concentration of calcium varies within the vein, with enriched zones outlining the geometry of individual calcite fibres. (d) Gradient in the vein (at a distance of about 500 μm from the wall) correlates with the CL-banding of the same sample. (e) Quartz selvage between vein and country crosscut by magnesium-rich plates, which are also abundant in the vein (chlorites). (f) Mg/Fe distribution clearly marks the selvage–wall interface. Three wall rock fragments can be found within the vein, along the zone where the Mn-content changes (corresponding change of the CL-intensity pattern).

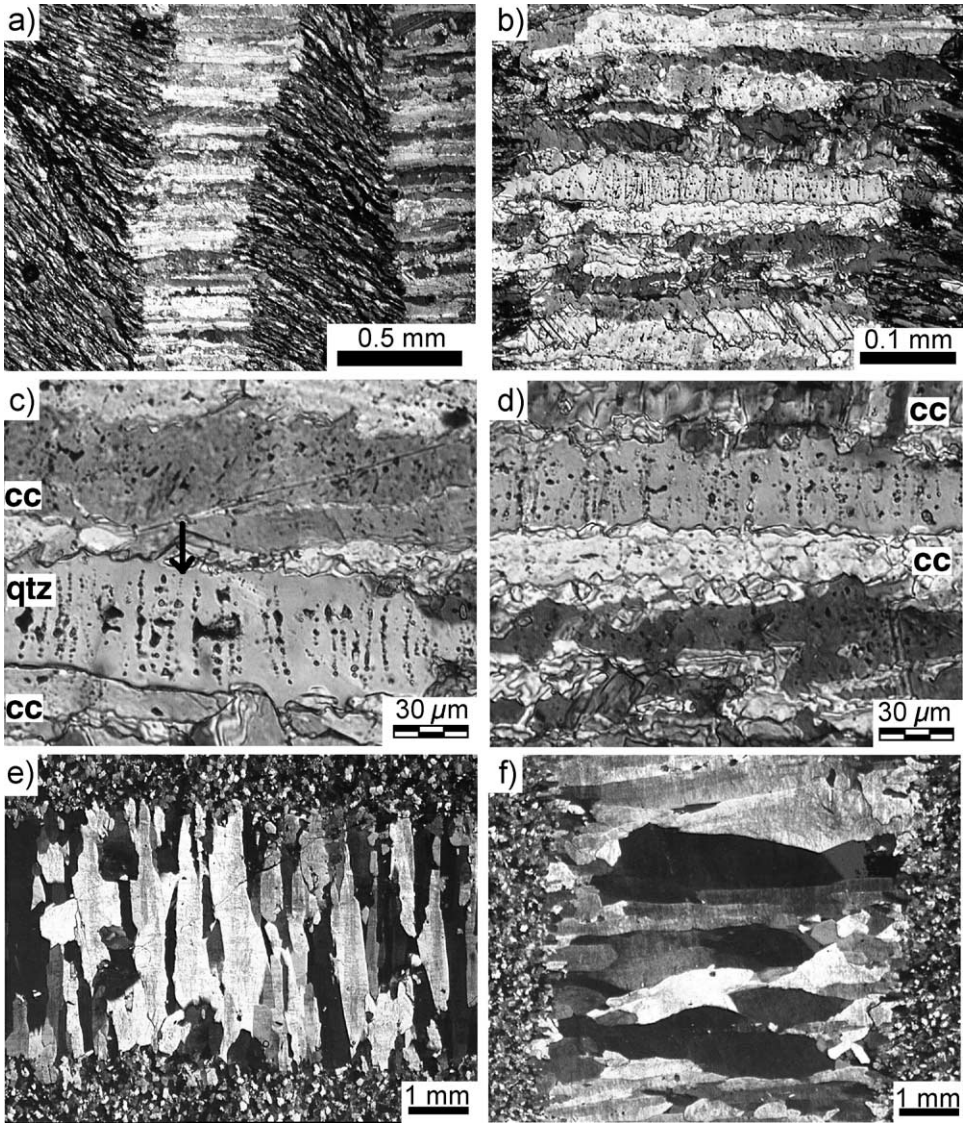

Fig. 9. Images of a bi-mineralic ataxial veins from the Morcles nappe, Switzerland (sample CH-980807-03). (a) Fibres connect foliation on both sides of the vein. (b) Solid inclusion bands are concentrated in quartz fibres. Fibre grain boundaries are serrated. The vein–wall interface is diffuse with quartz fibres being epitaxial overgrowths from quartz grains in the country rock. (c) Inclusion bands (arrow) do not continue into the adjacent calcite fibres. The length of individual inclusion bands seems to be constant along the fibre long axis, with the inclusion absent in a zone near the quartz fibre grain boundary. The vein–wall interface is located on the right hand side of the image. cc—calcite, qtz—quartz. (d) Example of solid inclusions arranged in bands in a quartz fibre, without such fabric in the adjacent calcite fibre. cc—quartz. (e) Mono-mineralic ataxial quartz veins from the Mosel valley, Germany. Quartz fibres cross the vein with a smooth grain boundary between adjacent fibres, sample Mo-16. (f) Epitaxial overgrowth along the wall shown by numerous small grains overgrown by their neighbours, especially on the left vein–wall interface of the image, sample Mo-21.

do not require a mechanical coupling of vein and wall when growing in a curved fibrous shape, if the crack increments are smaller than about 10 μm.

Country rock material protrudes into and across the vein. In contrast to selvage protrusions described above, these are not related to fibre curvature, and

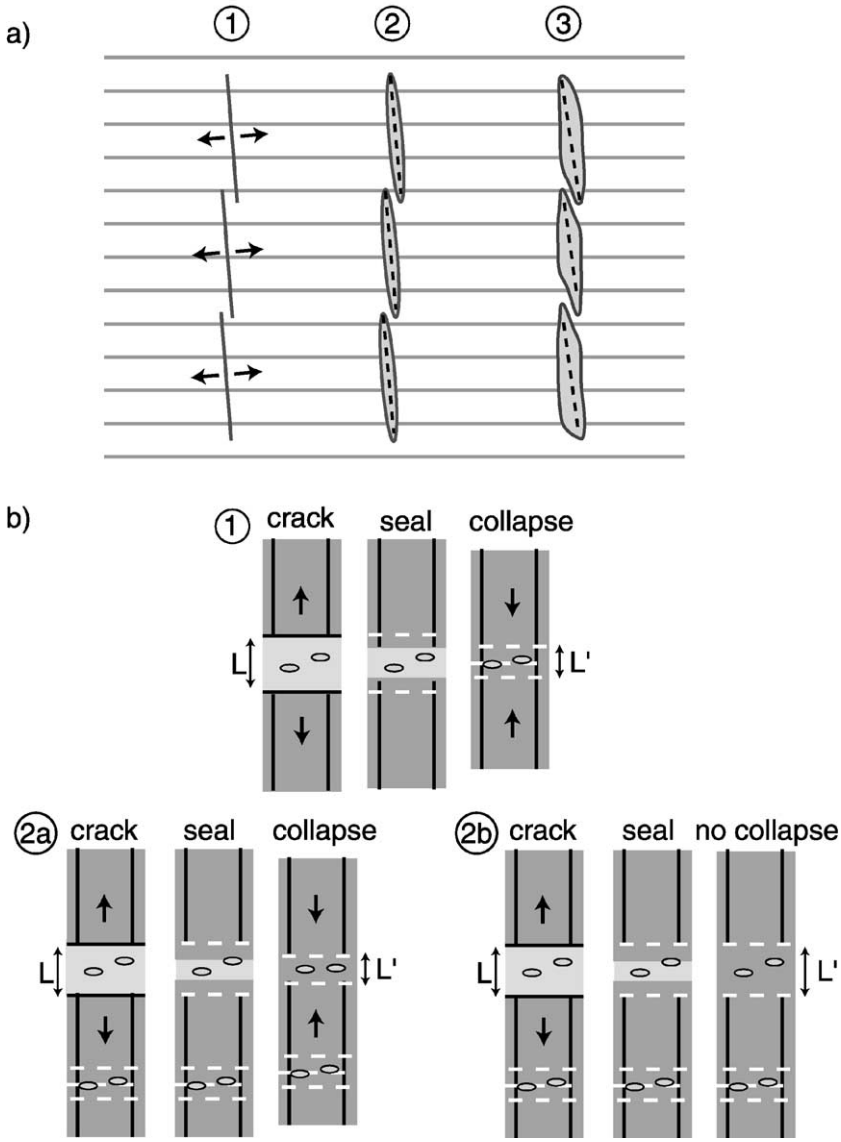

Fig. 10. (a) Early en-echelon fracture sets will be filled with vein material (1, 2). These veins will be finally arranged linearly during subsequent growth, with small bridges of country rock crossing the vein set. In such veins, the oldest part runs oblique to the wall (dashed line), which is also observed in CL (compare to Fig. 7g). (b) Sketch showing crack-seal increments with precipitation of fibre material and nucleation of secondary solid inclusions (dots) in a void. Fluid inclusion bands are marked with a dashed line. (1) A crack is opened, material precipitates and the fracture collapses as fluid pressure decreases. Fluid will be driven out of the fracture. A fracture collapse results in inclusion band spacing smaller than the initial crack. Note that other fluid inclusion bands might be formed during rapid grain growth. (2a) A second crack is opened, same history as in (1), with fluid inclusions formed only at initial void–wall interface. Fluid inclusion spacing of the fibre is smaller than the original crack. Fluid inclusion spacing of cracks (1) and (2a) cannot be correlated with the original crack width. (2b) If the crack is sealed without any collapse of the microstructure, fluid inclusion bands at the original interface correspond with the crack increment. Note that additional fluid inclusion bands formed by rapid grain growth will cause misleading results. The crack width L equals the inclusion spacing L'. Note that in all cases, solid inclusions cannot be used to deduce the crack opening.

contain deformation microstructures. CL-banding of adjacent veins ends obliquely at crossing protrusions (Fig. 7f,g). We interpret those country rock protrusions to be the result of deformation of relay zones between initially en-echelon veins during vein accretion. A schematic illustration of this is shown in Fig. 10a.

Inclusion bands, which might suggest a crack-seal mechanism, were not observed in our antitaxial samples. Inclusion trails of chlorites are irregularly distributed within the veins (Figs. 6c and 8). Thus, chlorites are interpreted as being dragged off from different sources at the vein–selvage interface. No evidence was found which suggests crack-sealing as the process forming antitaxial veins. Furthermore, regular inclusion bands and irregular inclusion trails were observed to form during continuous fibrous crystal growth in analogue experiments (Li, 2000; Means and Li, 2001). These might be a result of chemical oscillation during non-equilibrium processes (Allègre et al., 1981; Schneider and Münster, 1996; Hilgers, 2000, p. 61; Wiltschko and Morse, 2001), but certainly not of discrete crack events. Extrapolating this to natural fibrous veins, even inclusions aligned parallel to the vein–wall, would not be a criteria sufficient for the crack-seal mechanism (Hilgers, 2000; Wiltschko and Morse, 2001).

6.2. Ataxial veins

Bi-mineralic veins consist of optically continuous fibres without significant growth competition across the vein. If quartz and calcite minerals precipitated at different times, growth competition of the first aggregate would result in cavities that are later filled with the second mineral. This does not correspond with the fibrous morphology of both vein-filling minerals, and suggests simultaneous growth of both minerals. Kirschner et al. (1995) showed that calcite and quartz grew simultaneously in ataxial veins from the Morcles nappe, based on isotope studies.

Inclusion bands were observed to be concentrated in quartz fibres of bi-mineralic veins and are generally absent in adjacent calcite grains (similar observations by Kirschner et al., 1995, p. 1149). Such inclusion bands are frequently interpreted as indicator of a non-localised crack-seal process formed by repeated fracturing and growth at alternating different sites in the vein (Cox and Etheridge, 1983; Passchier and Trouw, 1996, pp. 133–136), with the spacing of inclusion bands correlated with the void opening increment. In our samples, it seems to be unlikely that a tectonic process would not leave a similar imprint of inclusions in adjacent calcite fibres, but only in quartz. Furthermore, the individual crack increment is almost impossible to determine from solid inclusion bands, as pointed out in Fig. 10b. Solid inclusions would only represent the crack increment, if they completely filled the void. Fluid inclusion bands have a potential to trace the crack increment, if the void did not collapse and, if only two inclusion bands are incorporated on either side of the crack (Fig. 10b). As mentioned above, other processes may also produce regularly spaced inclusion bands, without any cracking. The site of material accretion in ataxial veins is generally assumed to be determined by non-localised crack-sealing. However, potential indicators of this process, such as continuous inclusion bands, are absent in our bi-mineralic veins. If solid inclusions are fragments of the wall rock, accretion must have taken place at the diffuse vein–wall interface. Otherwise, wall rock fragments cannot be incorporated into the vein. Thus, the oldest part of the vein would be located in the centre of the microstructure, with precipitation of new material at the vein–wall interface (see Ramsay, 1980 p. 138 for similar interpretation).

In our mono-mineralic veins, inclusion bands crosscut all fibres. Growth competition takes place at the vein–wall interface, suggesting accretion of material within the vein. Such continuous fluid inclusion bands are generally referred to as indicators of a crack-seal process.

7. Conclusions

It has been shown that our antitaxial and bi-mineralic ataxial veins have grown with accretion of material at the vein–wall interface. No facets were formed, significant growth competition was absent and no nucleation of new grains took place during vein growth.

In the antitaxial calcite veins, a selvage of quartz and chlorite, and the calcite vein itself formed simultaneously. Chlorite inclusions were not incorporated into the vein microstructure by a crack-seal process. Bridges of country rock material formed as a result of

vein growth in an initial en-echelon arrangement. For at least some of our antitaxial veins, material was transported through the matrix and not along a fracture network.

Microstructural observations give no clear evidence of a crack-seal process in our antitaxial and bi-mineralic ataxial veins.

Acknowledgements

The microprobe analysis, carried out by Arne Willner (Ruhr-Universität Bochum), is gratefully acknowledged. Martin Burkhard, University of Neuchâtel, Switzerland organised an excellent introduction to the geology of the Morcles nappe and provided some valuable rock specimens. Some samples were provided by Frank Schrader, Halle, Germany. Alice Post made helpful comments on an early version of the manuscript. The manuscript greatly benefited from the comments by Mark Jessell and Dave Wiltschko. This project was funded by the Deutsche Forschungsgemeinschaft, grant Ur 64-1.

References

Allègre, C.J., Provost, A., Jaupart, C., 1981. Oscillatory zoning: a pathological case of crystal growth. Nature 294, 223–228.

Anonymous, 1814. Vein of fibrous limestone in chalk. Annals of Philosophy, London 4, 255–256.

Bons, P.D., 2000. The formation of veins and their micostructures. Journal of the Virtual Explorer, 2.

Bons, P.D., Jessell, M.W., 1997. Experimental simulation of the formation of fibrous veins by localised dissolution–precipitation creep. Mineralogical Magazine 61, 53–63.

Cox, S.F., 1987. Antitaxial crack-seal vein microstructures and their relationship to displacement paths. Journal of Structural Geology 9, 779–787.

Cox, S.F., 1995. Faulting processes at high fluid pressures: an example of fault valve behavior from the Wattle Gully fault, Victoria, Australia. Journal of Geophysical Research 100, 12841–12859.

Cox, S.F., Etheridge, M.A., 1983. Crack-seal fibre growth mechanisms and their significance in the development of oriented layer silicate microstructures. Tectonophysics 92, 147–170.

Dijk, P., Berkowitz, B., 1998. Precipitation and dissolution of reactive solutes in fractures. Water Resources Research 34, 457–470.

Dunne, W.M., Hancock, P.L., 1994. Paleostress analysis of small-scale brittle structures. In: Hancock, P.L. (Ed.), Continental Deformation. Pergamon, Oxford, pp. 101–120.

Durney, D.W., 1972. Deformation history of the western Helvetic nappes, Valais, Switzerland. PhD thesis, University of London, 327 pp.

Durney, D.W., Ramsay, J.G., 1973. Incremental strains measured by syntectonic crystal growths. In: de Jong, K.A., Scholten, R. (Eds.), Gravity and Tectonics. Wiley, New York, pp. 67–96.

Fisher, D.M., Brantley, S.L., 1992. Models of quartz overgrowth and vein formation: deformation and episodic fluid flow in an ancient subduction zone. Journal of Geophysical Research 97, 20043–20061.

Fisher, D.M., Brantley, S.L., Everett, M., Dzvonik, J., 1995. Cyclic fluid flow through a regionally extensive fracture network within the Kodiak accretionary prism. Journal of Geophysical Research 100, 12881–12894.

Grigorev, D.P., 1961. Ontogeny of Minerals. Israel Program for Scientific Translations, Jerusalem, pp. 1–250.

Hilgers, C., 2000. Vein growth in fractures-experimental, numerical and real rock studies. Publ. PhD-thesis, Shaker Verlag, Aachen, 104 pp.

Hilgers, C., Urai, J.L., 1999. Syntectonic antitaxial fibrous vein growth: inferences from the microstructure of natural samples. Göttinger Arbeiten zur Geologie und Paläontologie Sb4, 70–72.

Hilgers, C., Koehn, D., Bons, P.D., Urai, J.L., 2001. Development of crystal morphology during unitaxial growth in a progressively widening vein: II. Numerical simulations of the evolution of antitaxial fibrous veins. Journal of Structural Geology 23, 873–885.

Hulin, C.D., 1929. Structural control of ore deposition. Economic Geology 24, 15–49.

Kirschner, D.L., Sharp, Z.D., Masson, H., 1995. Oxygen isotope thermometry of quartz–calcite veins: unravelling the thermal–tectonic history of the subgreenschist facies Morcles nappe (Swiss Alps). GSA Bulletin 107, 1145–1156.

Kleber, W., 1983. Einführung in die Kristallographie, 15th edn. VEB Verlag, Berlin.

Koehn, D., Hilgers, C., Bons, P.D., Passchier, C.W., 2000. Numerical simulation of fibre growth in antitaxial strain fringes. Journal of Structural Geology 22, 1311–1324.

Li, T., 2000. Experimental growth of fibers and fibrous veins. Unpubl. PhD thesis, State University of New York at Albany, 420 pp.

Means, W.D., Li, T., 2001. A laboratory simulation of fibrous veins: some first observations. Journal of Structural Geology 23, 857–863.

Mügge, O., 1928. Ueber die Entstehung faseriger Minerale und ihrer Aggregationsformen. Neues Jahrbuch fur Mineralogie, Geologie und Paläontologie 58A, 303–348.

Mullin, J.W., 1993. Crystallization Butterworth-Heinemann, Oxford, 527 pp.

Nicholson, R., 1991. Vein morphology, host rock deformation and the origin of the fabrics of echelon mineral veins. Journal of Structural Geology 13, 635–641.

Nicholson, R., Ejiofor, I.B., 1987. The three-dimensional morphology of arrays of echelon and sigmoidal, mineral-filled fractures: data from north Cornwall. Journal of the Geological Society 144, 79–83.

Passchier, C.W., Trouw, R.A.J., 1996. Microtectonics. Springer, Berlin, 304 pp.

Ramsay, J.G., 1980. The crack-seal mechanism of rock deformation. Nature 284, 135–139.

Ramsay, J.G., Huber, M., 1983. The Techniques of Modern Structural Geology. Volume 1: Strain Analysis. Academic Press, London.

Rye, D.M., Bradbury, H.J., 1988. Fluid flow in the crust: an example from a Pyrenean thrust ramp. American Journal of Science 288, 197–235.

Schneider, F.W., Münster, A.F., 1996. Nichtlineare Dynamik in der Chemie. Spektrum, Heidelberg, 204 pp.

Simony, P.S., 1998. CTG Nuna field trip: transect of the Rocky Mountain fold and thrust belt, Canmore to Revelstoke. Field Guide, pp. 4–5.

Spencer, S., 1991. The use of syntectonic fibres to determine strain estimates and deformation paths: an appraisal. Tectonophysics 194, 13–34.

Taber, S., 1916. The origin of veins of the asbestiform minerals. Proceedings of the National Academy of Sciences 2, pp. 659–664.

ten Have, T., Heijnen, W., 1985. Cathodoluminescence activation and zonation in carbonate rocks: an experimental approach. Geologie en Mijnbouw 64, 297–310.

Urai, J.L., Williams, P.F., van Roermund, H.L.M., 1991. Kinematics of crystal growth in syntectonic fibrous veins. Journal of Structural Geology 13, 823–836.

Williams, P.F., Urai, J.L., 1989. Curved vein fibres: an alternative explanation. Tectonophysics 158, 311–333.

Wiltschko, D.V., Morse, J.W., 2001. Crystallization pressure versus "crack seal" as the mechanism for banded veins. Geology 29, 79–82.